

Approximate Critical Load of Cambered Double-Layered Grids by Shell Analogies

M.I. Ali, P.N. Khakina and F. Fan

School of Civil Engineering, Harbin Institute of Technology, 2453 P.O. Box 73,
Huanghe Road, Harbin 150090, China

Abstract: Studies have shown that design of double-layered grids based on classical theories may lead to unsafe design. For square-on-diagonal grids, the load carrying capacity is almost the same as the buckling load. Therefore the buckling load can be used as the critical load in the design. In this study, the non-linear behavior of the grids is considered using shell analogies to determine the critical load. By applying the theorem of study and energy to a dimple, an empirical formula to predict the buckling load of thin spherical shells was derived. Then using finite element modeling, post-buckling load was identified and used to calculate the value of constant C. It is observed that the buckling load is proportional to $t^{2.5}$, which gives a critical load close to what is observed in experiments and a more realistic load as compared to the Classical theory prediction. Load-deflection curves drawn for the grids and their equivalent continuum shells correlate closely showing that the findings are valid.

Keywords: Buckling, double-layered grid, equivalent continuum shell, finite element, single-layer grid, thin continuous shell

INTRODUCTION

Double-layered grids are commonly used to cover wide spans in floor, roof and bridge constructions because of their low mass, high rigidity and pleasant appearance. They have advantages such as load sharing, installation of services, robustness, modular components and regular geometry among others (Chilton, 2000). They are composed of interconnected grids of closely spaced members, which make them highly indeterminate thus having large number of redundant bars. It was believed that this inherent redundancy provided a large measure of safety against buckling because member buckling does not lead to collapse of the whole structure (Makowski, 1981) but collapse of some structures such as the roof of the Hartford Coliseum in 1987 (Sheidaii and Gholizadeh, 2006) which were designed based on this assumption has made it necessary to further examine the buckling behavior of the double-layered grids. In double-layered grids, collapse is progressive due to sequential failure of individual members or modules.

Buckling load of reticulated shells as investigated by Wright (1965) and Buchert (1976) is given by:

$$q_{cr} = C \frac{E}{R^2} t_m^{1/2} t_b^{3/2} \quad (1)$$

Experimental research has shown that Eq. (1) is equivalent to:

$$q_{cr} = CE \left(\frac{t_{eq}}{R} \right)^2 \quad (2)$$

If the network of the structure has regularity properties, it is generally possible to find a statically equivalent continuum and reduce the overall stability analysis of a grid structure to that of a continuous shell (Kollar and Dulacska, 1984). Continuum treatment has been used to analyze reticulated shells and double-layered lattice domes (GuoHua and ZhiWei, 2007; Yan *et al.*, 2009). Results by Kato and Mutoh (1996) lead to evaluation of buckling capacity of space frames in a similar way as that of ordinary practical design of columns in a framed building and of continuum shells. In this study, the continuum analogy method using shell analogies is used to determine the critical load of double-layered grids starting with thin continuous shells.

Empirical predictions of buckling load of thin spherical shells:

A double-layered grid can be cambered in both directions to give a spherical effect for water drainage which gives it a very small rise to span (f/L) ratio. Therefore in this study, a thin spherical shell with f/L = 1/40 is considered, which makes angle α to be very small as shown in Fig. 1:

$$r = R \sin \alpha \approx R \alpha \quad (3)$$

The depth of deformation:

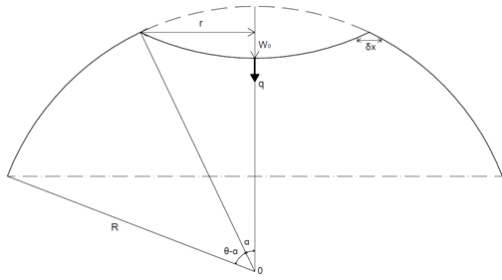


Fig. 1: Inversion of spherical shell by a radial force

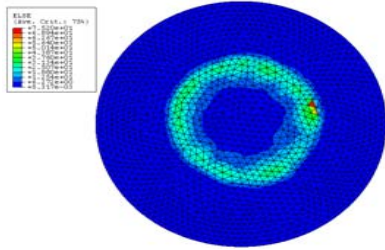


Fig. 2: Concentration of strain energy

$$W_0 = 2R(1 - \cos \alpha) \approx R\alpha^2 \quad (4)$$

Work done is given by the product of the radial force (q) and the volume of the inversed region:

$$W = 4/3 \pi q r^2 (w_0/2) \quad (5)$$

Substituting Eq. (3) and (4) into Eq. (5):

$$W = 2/3 \pi \alpha q r^3 \quad (6)$$

The strain energy is concentrated along the boundary layer (δx) of the inversed region as shown in Fig. 2. Landau and Lifshitz (1986) give the total strain energy as:

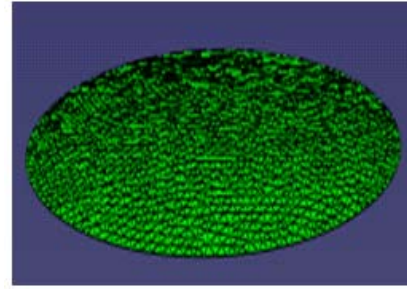
$$U = E t^3 (t/R)^{25} \quad (7)$$

Equating Eq. (6) and (7):

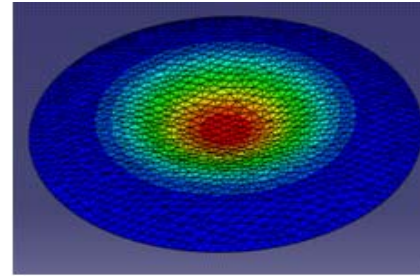
$$q_{cr} = CE(t/R)^{25} \quad (8)$$

where, C is a function of α , E is the Modulus of Elasticity, t is the thickness and R is the radius of curvature of the shell.

Finite Element (FE) modeling: Using FE analysis produces the optimum product; a product that is the least costly to produce, performs as intended and meets all of the specified requirements (Champion, 1992). Also, the structural behavior of shell structures during the whole loading process can be revealed by the load-deflection



(a) Geometry



(b) Initial geometrical imperfection

Fig. 3: Mild steel spherical shell; span (L) = 20 m, rise (f) = 0.5 m, thickness (t) = 0.02 m

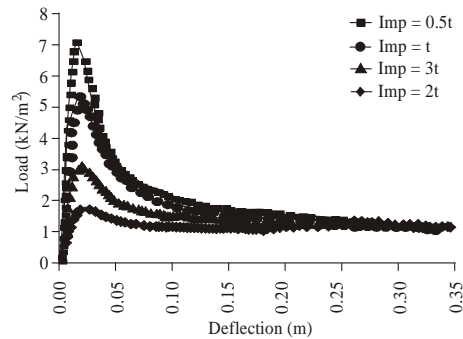


Fig. 4: Load-deflection curves of different magnitudes of initial geometrical imperfections

curves and the buckling load can be predicted with sufficient accuracy (Fan *et al.*, 2010). The concepts of nonlinearity and imperfection sensitivity gives an explanation for the buckling performance of thin shell structures (Zhu *et al.*, 2002; Zhou *et al.*, 2010), therefore using the post-buckling load which is based on the non-linear behavior to determine the critical load gives a more realistic prediction. The post-buckling load is taken from the 'plateau' on the load-deflection curves where the curves tend to meet for the shells or the point of intersection of the curves for the grids so as to eliminate the initial geometrical imperfections.

Post-buckling load: The angle θ is can be determined by the f/L ratio and which is then used to find the value of α . Therefore by changing the values of f/L , the relationship of C and α can be determined. Using the Riks method (Hibbitt, 2000) with magnitude of the initial geometrical imperfection $0.5t$, t , $2t$ and $3t$, respectively, FE modeling was done on a spherical shell with a very small value of θ to make the shell to be almost equivalent to grids which are cambered in both directions and supported around all edges as shown in Fig. 3. The load-deflection curves are shown in Fig. 4.

It is observed that the initial buckling of the shell is sensitive to the initial geometrical imperfection while the post-buckling load is little influenced because irrespective of the magnitude of the imperfection; the curves tend to meet. Basing on this load, it is possible to find the value of C which is a function of α because imperfections have been eliminated.

Value of C: The major factors that contribute to overestimation of the buckling load by the classical buckling theory are:

- Geometric parameters
- Material parameters
- Boundary conditions
- Pre-buckling deformations
- Geometric imperfections (Teng, 1996; Forasassi and Frano, 2007)

The use of the post-buckling load eliminates all types of imperfections. Studies have shown that buckling does not depend essentially on the type of boundary conditions (Barski, 2006) and the effect of pre-buckling deformations is very small if any. Therefore, C should be a function of some geometrical parameters which determine the value of α because the material parameters are kept constant. The geometrical parameters are R , t , L and f . A study by Khakina *et al.* (2011) gave the value of C in terms of L and f while keeping t constant.

BUCKLING LOAD FOR SINGLE-LAYER GRIDS USING CONTINUUM ANALOGY METHOD

Buckling load equation for single-layer grids: With reference to Narayanan (2006), a reticulated shell of triangular-type pattern with equilateral triangular grid has an equivalent membrane thickness of:

$$t_m = 2A / a\sqrt{3} \tag{9}$$

and with an effective bending thickness of:

$$t_b = (9\sqrt{3}I/a)^{1/3} \tag{10}$$

where, a is the length of the bar, A the cross-sectional area and I the moment of inertia.

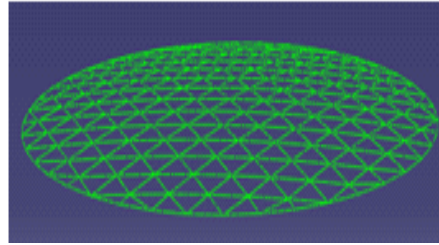


Fig. 5: Single layer grid cambered in all in two directions and support around all edges

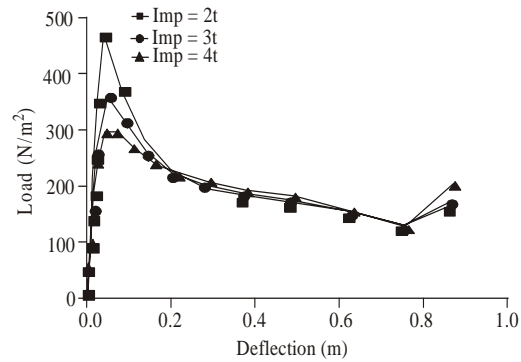


Fig. 6: Load-deflection curves for single-layer grid

As observed from studies, the equivalent of Eq. (1) is:

$$q_{cr} = CE_{eq}(t_{eq}/R)^2 \tag{11}$$

In this study, the equivalent of Eq. (8) will be:

$$q_{cr} = CE(t_{eq}/R)^{25} \tag{12}$$

By conducting FE modeling for several single-layer reticulated shells, it is observed that:

$$t_{eq} = t_m^{0.2} t_b^{0.8} \tag{13}$$

Equating the corresponding elements in the first row and first column of the membrane rigidity of continuous shells and tensile rigidity matrix of grids:

$$t_m = 3\sqrt{3}A(1-\nu^2)/4a \tag{14}$$

The value obtained by Eq. (9) and (14) is the same. Equating the corresponding elements in the first row and first column of the bending rigidities of the continuous shells and grids:

$$t_b = \left[\frac{12\sqrt{3}I(1-\nu^2)}{4a} \left(3 + \frac{GI_t}{EI} \right) \right]^{1/3} \tag{15}$$

Substituting for values of t_m and t_b :

Table 1: Values of the buckling load of single-layer grid from different sources.

| Source | Equation | q _{cr} value (N/m ²) |
|--|--|---|
| Pozo and Pozo (1979) | $q_{er} = 0.247 E/R^2 t_m^{1/2} t_b^{3/2}$ | 149 |
| Current study | $q_{er} = 12 E(t_{eq}/R)^{2.5}$ | 126 |
| FE modeling for single-layer grid and its equivalent | ABAQUS | 129 |

Table 2: Values of the critical load of double-layered grid from different sources

| Source | Equation | Critical load (kN/m ²) |
|----------------------|--|------------------------------------|
| Current study | $q_{er} = 12 E(t_{eq}/R)^{2.5}$ | 44.5 |
| Pozo and Pozo (1979) | $q_{er} = 0.247 E/R^2 t_m^{1/2} t_b^{3/2}$ | 34.6 |
| Buchert (1976) | $q_{er} = 0.365 E/R^2 t_m^{1/2} t_b^{3/2}$ | 51.1 |

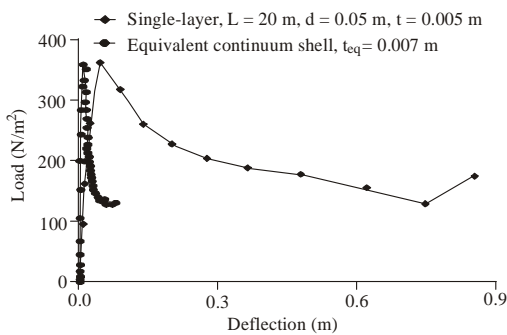


Fig. 7: Load-deflection curves for the equivalent continuum shell

$$t_{eq} = \left[\frac{6A^{0.7} I}{a^{1.7}} \left(3 + \frac{GI_t}{EI} \right) \right]^{0.27} \quad (16)$$

Validation of the buckling load equation: To validate Eq. (12), FE modeling for a single-layer grid of L = 20 m with equilateral triangular grids using seamless steel tubes of Ø = 50 mm and thickness = 5 mm was done as shown in Fig. 5. The thickness t_{eq} of its equivalent continuum shell was calculated using Eq. (16) and FE modeling for the shell with same L was done. The load-deflection curves for the single-layer grid are shown in Fig. 6. Comparison curves for both the grid and its equivalent continuum shell are shown in Fig. 7. The curves show that the grid and its equivalent continuum shell have different deflections but the same initial buckling load and post-buckling load. The critical buckling load as observed from various sources is shown in Table 1. The load as given by the empirical formula and that from FE modeling is almost the same and close to experimental load by Pozo and Pozo (1979) which is a proof that the equation is valid.

Critical load for double-layered grids: A study by Supple and Collins (1981) showed that the value of the post-critical slope of the member collapse curve greatly influenced the overall structural collapse of the structure. Basing on the continuum analogy method, the critical load

equation for the double-layered grid is the same as buckling load equation of a single-layer grid but with different values of effective membrane thickness and effective bending thickness. Experiments have shown that the effective membrane thickness for double-layered grids is roughly double that of the single-layer grids. A double-layered grid with each grid having an equivalent membrane thickness given by Eq. (9) has an equivalent membrane thickness of:

$$t_m = 2A/av\sqrt{3} \quad (17)$$

with an effective bending thickness of:

$$t_b = 2 \left\{ \frac{2A\sqrt{3}}{a \left[\frac{d}{2} \right]^2} \right\}^{1/3} \quad (18)$$

From Eq. (1) and (2), it is observed that:

$$t_{eq}^2 = t_m^{1/2} t_b^{3/2} \quad (19)$$

Substituting Eq. (17) and (18) into Eq. (19) and solving:

$$t_{eq} = 4(A/ad)^{0.5} \quad (20)$$

where, A is the cross-sectional area of the bar, a is the length of the bar and d is the distance between the two grids.

To validate the empirical formula for calculating the critical load of double-layered grids, an example of a grid with triangular pattern of L = 20 m, d = 1 m, a = 1.67 m, Ø = 0.05 m, t = 0.005 m is used. Using Eq. (20), t_{eq} = 0.08 m. The load from different sources is shown in Table 2.

The critical load derived in the study is within the range of critical loads in previous studies. Therefore, the empirical formula is valid.

CONCLUSION

It is observed in this study that the buckling load is proportional to t^{2.5}. With this observation, the continuum analogy method has been used to determine the critical load of double-layered grids. The buckling load of thin spherical continuous shells was derived basing on the theorem of study done and the strain energy released during the inversion of the shell. The critical buckling load of single-layer grids was determined using the post-buckling load from load-deflection curves. Finally, the critical load of double-layered grids was determined using the shell analogies. The existing empirical formulae used to calculate the buckling load of single-layer grids and double-layered grids are the same but with different t_m and t_b. In this study, the derived empirical equation is also the same but with different values of t_{eq}. The classical theory

overestimates the buckling load (Prevost *et al.*, 1984) therefore the observed load will give a more realistic prediction because it gives a value within the range of experimental critical loads.

REFERENCES

- Barski, M., 2006. Optimal design of shells against buckling subjected to combined Loadings. *Str. Multidisc Optim*, 31: 211-222.
- Buchert, K.P., 1976. Shell and Shell-like Structures. In: Johnston, B.G., (Ed.), *Guide to Stability Design Criteria for Metal Structures*. 3rd Edn., Wiley, New York.
- Champion, E.R., 1992. *Finite Element Analysis in Manufacturing Engineering*. APC-Based Approach, McGraw-Hill, Inc., New York.
- Chilton, J., 2000. *Space Grid Structures*. Architectural Press, Oxford.
- Fan, F., Z. Cao and S. Shen, 2010. Elasto-plastic stability of single-layer reticulated shells. *Thin Walled Str.*, 48: 827-836.
- Forasassi, G. and R. Frano, 2007. Curved thin shell buckling behavior. *J. Achievements Mater. Manuf. Eng.*, 23(2): 55-58.
- GuoHua, N. and L. ZhiWei, 2007. Nonlinear analysis of imperfect squarely-reticulated shallow spherical shells. *Sci. China Ser G*, 50: 109-117.
- Hibbitt, 2000. *ABAQUS User's Manual Version 6.1*. Karlsson and Sorensen Inc., Pawtucket.
- Kato, S. and I. Mutoh, 1996. Influence of local imperfections on buckling strength of reticulated shells. *J. Struct. Eng.*, 42(a): 147-158.
- Khakina, P.N., M.I. Ali, E.N. Zhu, H.Z. Zhou and B.H. Moula, 2011. Effect of the rise/span ratio of a spherical cap shell on the buckling load. *WASET*, 80: 446-452.
- Kollar, L. and E. Dulacska, 1984. *Buckling of Shells for Engineers*. John Wiley and Sons, London.
- Landau, L.D. and E.M. Lifshitz, 1986. *Theory of Elasticity*. Butterworth-Heinemann, Oxford.
- Makowski, Z.S., 1981. Review of the Development of Various Types of Double-Layer Grids. In: Makowski, Z.S., (Ed.), *Analysis, Design and Construction of Double-Layer Grids*. Applied Publishers Ltd., London.
- Narayanan, S., 2006. *Space structures: Principles and Practice*. Multi-Science Publishing Co. Ltd., Brentwood.
- Pozo, F.F. and V.F. Pozo, 1979. Buckling of ribbed spherical shells. *Proceeding of IASS Congress*, 1: 199-222.
- Prevost, J.H., D.P. Billington, R. Rowland and C.C. Lim, 1984. Buckling of spherical dome in a centrifuge. *Exp. Mech.*, 24(3) 203-207.
- Sheidaii, M.R. and S. Gholizadeh, 2006. An investigation into the collapse behavior of double-layer space trusses using neural networks. *Proceeding of ICCE*, Tehran.
- Supple, W.J. and I. Collins, 1981. Limit State Analysis of Double-Layer Grids. In: Makowski, Z.S. (Ed.), *Analysis, Design and Construction of Double-Layer Grids*. Applied Science Publishers Ltd, London.
- Teng, G. J., 1996. Buckling of thin shells: Recent advances and trends. *Appl. Mech.*, 49: 263-274.
- Wright, D.T., 1965. Membrane forces and buckling in reticulated shells. *J. Struct. Div. ASCE*, 91: 173-201.
- Yan, C., Y. Taniguchi and S. Yoshinaka, 2009. Effect of Member Layout on Elastic Buckling Behavior for Square-and-Diagonal Double-Layer Lattice Domes. *Proceeding of IASS Symposium*, Valencia.
- Zhou, H.Z., F. Fan and E.C. Zhu, 2010. Buckling of reticulated laminated veneer lumber shells in consideration of the creep. *Eng. Str.*, 32: 2912-2918.
- Zhu, E., P. Mandal and C.R. Calladine, 2002. Buckling of thin cylindrical shells: An attempt to resolve a paradox. *Int. J. Mech. Sci.*, 44: 1583-1601.